

# Design Refinement and Improvement of Flux Switching Machine with Outer-Rotor Configuration

<sup>1</sup>M. Z. Ahmad, <sup>2</sup>E. Sulaiman, <sup>3</sup>Z. A. Haron, and <sup>4</sup>F. Khan

Dept. of Electrical Power Engineering  
Faculty of Electrical & Electronic Engineering  
Universiti Tun Hussein Onn Malaysia  
Johor, Malaysia

<sup>1</sup>zarafi@uthm.edu.my, <sup>2</sup>erwan@uthm.edu.my, <sup>3</sup>zainalal@uthm.edu.my, and faisalkhan@ciit.net.pk

**Abstract** — Flux switching machines (FSMs) become an attractive research topic recently due to their distinct advantage of single piece robust rotor structure and suitable for high speed applications. In addition, the machines have a capability to produce high torque and power density similar as interior permanent magnet synchronous machine (IPSM) that conventionally employed in electric vehicles (EVs). This paper describes design refinement and improvement of 12-Slot 10-Pole FSM with outer-rotor configuration. In this study, JMAG-Designer ver. 13.1 is used as two dimensional (2-D) Finite Element Analysis (FEA) solver. Under some design restrictions and specifications for the target electric vehicle (EV) drive, the performances of the machine show good improvement in term of torque and power density. Finally, it is expected that the proposed machine has ability to achieve the target performances by implementing 'deterministic optimization design approach'.

**Keywords**-component; Outer-rotor hybrid excitation flux switching machine; field excitation coil; electric vehicle

## I. INTRODUCTION

In this decade, a lot of government agencies and private companies put more attention on preventing global warming issue. As well known, vehicle emission is among of the factor that contributes on this issue and it conventionally come from internal combustion engine (ICE) vehicles. They did a lot of research to help reducing this issue with practical approaches. In automotive field, the most practical solution to avoid emission is implementing fully electric vehicle (EV) widely. The zero-emission vehicle has a great potential to dominate the future vehicle market due to the constraint regulations have been made on vehicle emission and fossil fuels. On a EVs system, the propulsion system is among of the essential parts to propel the vehicle. In-wheel direct drive is the latest technology on EV propulsion system which giving advantages of low noise, high efficiency, and less maintenance due to the elimination of gearing and belting system as conventionally employed in single motor drive of EV. Previously, the most suitable machine for direct drive application is permanent magnet (PM) brushless machine that commonly known as permanent magnet synchronous machine (PMSM). This is due

to their distinguish advantages of high torque density, excellent efficiency, and overload capability.

In recent years, flux-switching motors (FSMs) have been extensively investigated due to their several advantages of robust rotor structure, higher torque density, and efficiency. With all the excitation sources such as PMs and coil windings are located on the stator body, the generated heat on the stator along the operation is easily dissipated through a cooling system management. On the other hand, with the machine only has a piece of salient rotor, it's like a combination advantages of PMSM and switched reluctance motor (SRM). The first single phase FSM was introduced in 1955 as an alternator and used for airborne application. Then, a three-phase FSM has been developed in 1997 with 12-slot 10-pole configuration. Afterward, a lot of improvement and development have been made on FSM and various structure of FSM was proposed for wide range of application such as in domestic electric power tools, wind power generation, automotive, as well as for aerospace applications. There are three categories of FSMs and can be classified into permanent magnet (PM) FSMs, hybrid excitation (HE) FSMs, and field excitation (FE) FSMs. Both PMFSMs and FEFSMs have only single excitation flux source either come from PM or FE coil, while in HEFSM the magnetic flux source is generated from PM and FECs. The HEFSM and FEFSM has additional advantage of variable flux control capability when compared with PMFSM and more fortunately it can be used at various speed conditions.

In the most researches done on FSMs, the attention given from industrial and academic researchers are on conventional inner-rotor machine, only recently several researchers are focusing on outer-rotor configuration. The outer-rotor structure is more suitable for direct drive applications and potentially can be applied for in-wheel drive of EV. The first outer-rotor PMFSM has been introduced in 2009 and specially designed for urban electric vehicle. Then, in 2012 field wound segmented outer-rotor FSM and outer-rotor HEFSM has been proposed for aerospace and EV applications, respectively. This paper describes design refinement and improvement of 12-slot 10-pole HEFSM with outer-rotor configuration that firstly has been proposed by the authors as reported in []. Based on two-dimensional (2-D) analysis, the performances of the machine

---

M.Z. Ahmad is with Universiti Tun Hussein Onn Malaysia, Johor, 86400 Malaysia (e-mail: zarafi@uthm.edu.my)

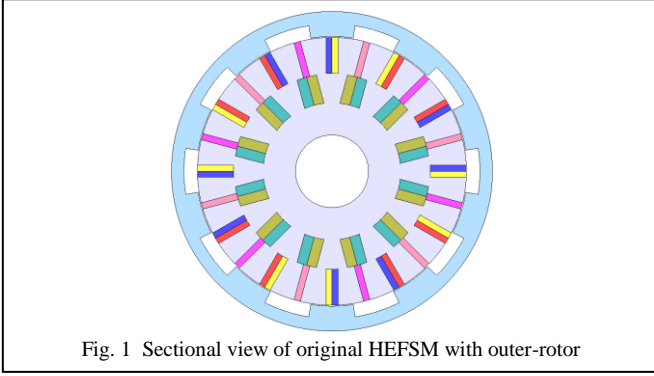


Fig. 1 Sectional view of original HEFSM with outer-rotor

are analyzed and investigated. The structure of the original proposed machine is shown in Fig. 1.

The rest of the paper consists of the following; Section II will discuss the design requirements, restrictions, and specifications of the proposed motor. The design improvement methodology is presented in Section III, while the results and performances of the improved design motor are given in Section IV. Finally, Section V gives a conclusion on this design refinement and improvement study.

## II. DESIGN REQUIREMENTS, RESTRICTIONS AND SPECIFICATIONS

The design requirements, restrictions and specifications for the proposed HEFSM with outer-rotor configuration are similar as interior permanent magnet synchronous motor (IPMSM) employed in LEXUS RX400h and listed in Table I. The target maximum torque and power are set to be more than 333 Nm and 123 kW, respectively. The PM weight is set to 1.0 kg, which less by 0.1 kg compared with the PM used in IPMSM. The corresponding electrical restrictions to the inverter such as maximum DC bus voltage and maximum inverter current are set to 650 V and 360 A<sub>rms</sub>, respectively, while the limit of both armature current density,  $J_a$  and FEC current density,  $J_e$  is set to 30 A/mm<sup>2</sup>. The proposed motor has very simple structure where the shape of each component is in rectangle form and all coils are wound in concentrated form. In addition, it offers non-overlap winding between the FEC and armature coil that makes shorter end winding and can contribute to reduce copper loss effect. The target weight of the proposed motor is set to be less than 30 kg. Therefore, the proposed motor is expected to achieve the maximum torque density and power density of 11.1 Nm/kg and 4.1 kW/kg, respectively.

In this proposed motor, for the motor rotation through 1/10 of a revolution, the flux linkage of armature has one periodic cycle and thus, the frequency of back-emf induced in the armature coil is ten times the mechanical rotational frequency. In general, the relation between the mechanical rotation frequency,  $f_m$  and the electrical frequency,  $f_e$  for the proposed machine can be expressed by

$$f_e = N_r \cdot f_m \quad (1)$$

where  $f_e$  is the electrical frequency,  $f_m$  is the mechanical rotation frequency and  $N_r$  is the number of rotor poles respectively.

TABLE I. OUTER-ROTOR HEFSSM DESIGN RESTRICTIONS AND SPECIFICATIONS

Descriptions	IPMSM	Outer-rotor HEFSM
Max. DC-bus voltage inverter (V)	650	
Max. inverter current (A <sub>rms</sub> )	360	
Max. current density in armature coil, $J_a$ (A <sub>rms</sub> /mm <sup>2</sup> )	30	
Max. current density in FEC, $J_e$ (A/mm <sup>2</sup> )	30	
Motor diameter (mm)	264	
Motor stack length (mm)	70	
Shaft diameter (mm)	60	
Air gap length (mm)	0.8	
Armature coil slot	12	
FEC slot	12	
Armature coil turn	7	
FEC turn	44	
PM weight (kg)	1.1	1.0
Total weight of machine (kg)	35	<30
Maximum speed (r/min)	12,400	>12,400
Maximum torque (Nm)	333	>333
Maximum power (kW)	123	>123

The commercial FEA package, JMAG-Designer ver.12.0, released by Japan Research Institute is used as 2D-FEA solver in this design. The material used for PM is NEOMAX 35AH with residual flux density and coercive force at 20 ° are 1.2T and 932 kA/m, respectively. Whereas for the stator and rotor body, the material used is electrical steel, 35H210.

Initially, the 30° mechanical angle of stator yoke is designed with the following assumptions;

- The inner radius is set to 30 mm for the motor's shaft while the outer radius is set to 110.6 mm, making the stator depth of 80.6 mm which is 61% of 132 mm motor radius and within the range of general machine split ratio,
- The PM volume is set to 1.0 kg, which is less 0.1 kg compared with the PM used in IPMSM. The reason is to reduce the PM cost due to the increasing price of PM since 2011,
- By expecting that the higher of the PM depth will give more flux to flow and increase the motor performances, therefore the PM depth is set to 29.7 mm which is approximately one third of stator depth. However, demagnetization effect needs to be taken into consideration when higher PM depth is applied especially at the edge of the PM,
- The FEC slot area is set to 197.01 mm<sup>2</sup> to give a maximum current density,  $J_e$  of 30 A/mm<sup>2</sup> with 44 turns of FEC winding. The FEC slot depth is less than the PM depth to give an appropriate distance between two FEC slots area for the flux to flow in this area,
- The depth of armature slot area is set similar to the PM depth in order to avoid overlapping between armature coil winding and FEC winding. Therefore, it is expected that the motor will use shorter coil end winding and so reduces copper loss effect.

Besides that, the initial for 36° mechanical angle of rotor iron is designed with the following assumptions;

- (i) The air gap is set similar as the IPMSM which is 0.8 mm, hence the inner rotor radius becomes 111.4 mm and this gives a rotor depth of 20.6 mm,
- (ii) The rotor pole depth is set to 10.3 mm which is half of the rotor iron depth to allow the flux flow easily through the outer rotor pitch,
- (iii) The rotor pole arc width is set to be similar with the rotor pole gap to allow optimal flux flows into the rotor pitch.

### III. IMPROVED DESIGN METHODOLOGY

Initially, the performances of the original structure machine as shown in Fig. 1 have been computed and evaluated. The results obtained show that the maximum power and torque of original design machine is 70.4 kW and 205.6 Nm, respectively. Since, it is far from the target performances, it is required to be optimized by implementing parameters refinement and optimization.

Thus, the motor parameters are divided into two categories, namely, those related to stator iron core and rotor iron core. On the stator iron core, it is subdivided into three components which are the PM shape, FEC slot shape, and armature slot shape. The rotor parameters involved are the inner rotor radius ( $D_1$ ), rotor pole depth ( $D_2$ ), and rotor pole arc width ( $D_3$ ). The distance between airgap and PM is ( $D_4$ ). The PM slot shape parameters are the PM depth ( $D_5$ ), and the PM width ( $D_6$ ), while for the FEC slot parameters are FEC slot depth and FEC slot width, ( $D_7$ ) and ( $D_8$ ) respectively. Finally, the armature coil parameters are armature coil slot depth ( $D_9$ ) and the armature coil slot width ( $D_{10}$ ). The motor design parameters, from  $D_1$  to  $D_{10}$  are demonstrated in Fig. 2. Based on the motor parameters have been identified, the deterministic design optimization method is used and implemented using 2-D FEA solver to obtain the optimal performances of the proposed motor at different . Since, the torque is proportional to the square of rotor radius  $D_1$  under the condition that the specific electric and magnetic loadings are kept constant; the rotor radius  $D_1$  is firstly treated as the most sensitive parameter to increase the torque. On the other hand, the others parameters from  $D_2$ - $D_{10}$  are fixed but must be shifted according to the displacement of  $D_1$ . Then, with the optimal value of  $D_1$  that producing the highest torque, the rotor pole width and depth  $D_2$  and  $D_3$ , respectively, are adjusted in order to get the optimal parameters.

Consequently, the second step is executed by changing the parameters of PM  $D_4$ ,  $D_5$ , and  $D_6$  while keeping  $D_1$ ,  $D_2$ , and  $D_3$  at optimal value. Then, the best combination of  $D_4$ ,  $D_5$ , and  $D_6$  are selected to give the optimal performance in terms of torque. The same procedures are applied for the rest machine parameters up to  $D_{10}$ . The procedures are repeated until the maximum torque and power are satisfied. In summary, the motor parameters  $D_1$  to  $D_{10}$  are changed repeatedly until the target performances of torque and power are achieved. In this study, the initial design and improved design parameters of the proposed outer-rotor HEFSM are depicted in Table II. The improved design structure of outer-rotor HEFSM is illustrated in Fig. 3. In this design improvement, the simple structure of

the proposed motor is retained and overlap between armature coil and FEC coil windings avoided. However, the shape of the armature coil slot became a trapezoidal shape to allow the flux flow to the rotor smoothly and reduced flux leakage.

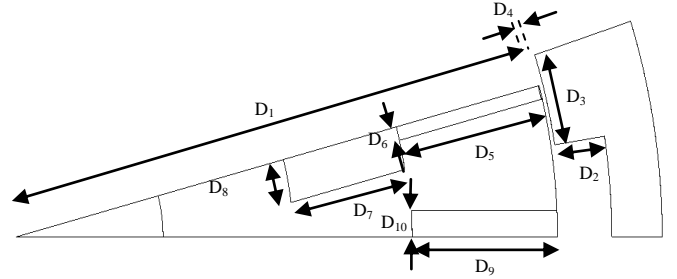


Fig. 2 Design parameters defined as  $D_1 - D_{10}$

TABLE I. THE DESIGN PARAMETERS FOR THE PROPOSED ORHEFSM

Parameter	Description	Initial	Improved
$D_1$	Rotor inner radius (mm)	110.6	108.4
$D_2$	Rotor pole depth (mm)	10.3	12.3
$D_3$	Rotor pole arc width ( $^\circ$ )	9	13
$D_4$	Distance between airgap and PM (mm)	0.2	0
$D_5$	PM depth (mm)	30	20
$D_6$	PM width (mm)	2.63	3.95
$D_7$	FEC slot depth (mm)	23.88	40.60
$D_8$	FEC slot width (mm)	8.25	5.03
$D_9$	Armature coil slot depth (mm)	29.7	17.2
$D_{10}$	Armature coil slot width (mm)	4.95	8.14

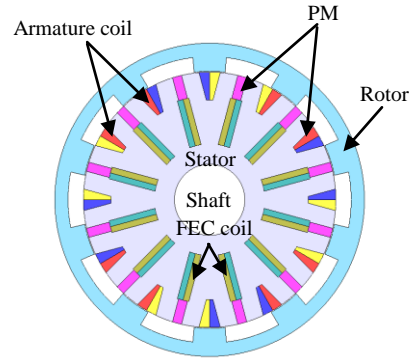


Fig. 3 Improved design structure of ORHEFSM

## IV. RESULTS AND PERFORMANCES OF THE IMPROVED DESIGN

### A. Open circuit analysis

Initially, the magnetic flux linkage in open circuit condition of the proposed motor is investigated. The flux linkage of the initial and improved design at various condition of  $J_e$  is plotted in Fig. 4 and Fig. 5, respectively. From these two figures, it is clearly demonstrated that the magnitude of flux linkage of the improved design at maximum  $J_e$  of 30 A/mm<sup>2</sup> has increased from 0.03 Wb to 0.05 Wb. Thus, it is

expected that the performances of the machine will have enhancement.

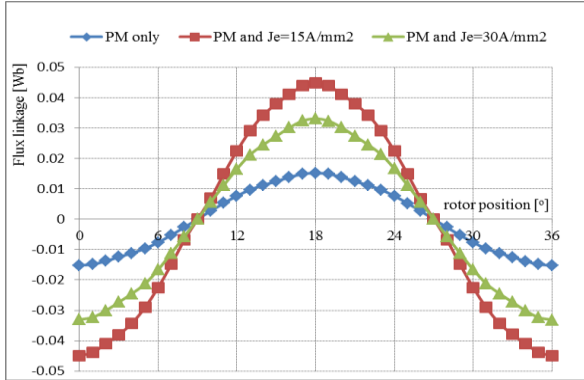


Fig. 4 U-phase flux linkage at various conditions of  $J_e$  for initial design motor

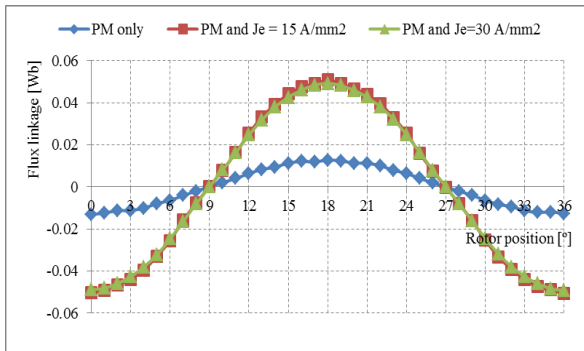


Fig. 5 U-phase flux linkage at various conditions of  $J_e$  for improved design motor

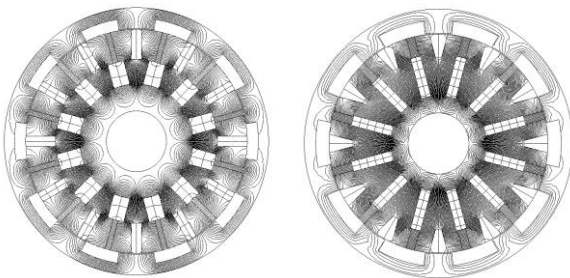


Fig. 6 Flux path of PM in open circuit condition (a) Initial design  
(b) Improved design

Besides that, the field distribution for PM of initial design and improved design ORHEFSM are also investigated and the results obtained are shown in Fig. 6. From the diagram, it shows that for initial design 50 % of PM flux flows to the rotor causing higher generated induce voltage, while for the improved design, there is a great reduction of flux flow to the rotor which is approximately 10 % of generated flux. Consequently, it provides less cogging torque and reduces the amplitude of back-emf at open circuit condition. The comparison of back-emf of initial and improved design ORHEFSM at the speed of 3000 r/min is illustrated in Fig. 9. It is clearly shown that the amplitude of back-emf for the

improved design motor has significantly been reduced from 82.44 V to 70.78 V, which is approximately 14% reduction. In addition, the back-emf of the improved designed motor looks more sinusoidal compared with the initial design motor.

Furthermore, the cogging torque of the improved design ORHEFSM compared with the initial design is exemplified in Fig. 10. From the graph, the improved design motor shows great reduction in peak-to-peak cogging torque ripple where it has reduced 76.7% from 10.2 Nm to 3.6 Nm. Therefore, it is expected that the motor has the potential to be applied for high speed applications.

### B. Load Analysis

In load analysis, the torque versus FEC current density at maximum  $J_a$  and the average torque of the initial and improved design is compared and plotted as depicted in Fig. 11 and Fig. 12, respectively. The average maximum torque obtained for the initial design is 205.6 Nm, whilst the improved design ORHEFSM is 271.5 Nm. It is shown that the improved design motor has produced higher torque with 32% improvement compared to initial design motor and has achieved 81.5 % from the target value. The torque obtained at various conditions of  $J_e$  and  $J_a$  for improved design ORHEFSM are also analyzed and plotted as shown in Fig. 13. From the diagram, when  $J_a$  is set at maximum of 30 A<sub>rms</sub>/mm<sup>2</sup>, the torque keeps increasing as  $J_e$  is increased from 0 A/mm<sup>2</sup> to 30 A/mm<sup>2</sup>. Whereas, when  $J_a$  is set between 10 A<sub>rms</sub>/mm<sup>2</sup> to 25 A<sub>rms</sub>/mm<sup>2</sup>, the output torque is maintained constant for  $J_e$  greater than 25 A/mm<sup>2</sup>. This phenomenon is due to the flux saturation effect and an investigation on magnetic flux distribution is required to overcome the problem.

Consequently, with the improvement of the maximum torque of the improved design ORHEFSM, the maximum power also has been increased and obviously it has achieved beyond the target value. Previously, for the initial design motor the maximum power achieved was 70.4 kW, while for the improved design motor, it has increased dramatically to 143.6 kW, since the target maximum power is only 123 kW. Although, the target performance for the maximum torque was not achieved, further design refinement and optimization will be conducted in future and it is expected the target performance will be achieved.

## V. CONCLUSION

In this paper, design refinement and improvement study of 12-Slot 10-Pole HEFSM with outer-rotor configuration have been presented. The simulated performances of the proposed motor has achieved 81.5% from the target value of maximum torque, whilst for the maximum power has achieved beyond the target performances. Thus, it is expected that the target performance for the maximum torque can be achieved by further design refinement and optimization in future.

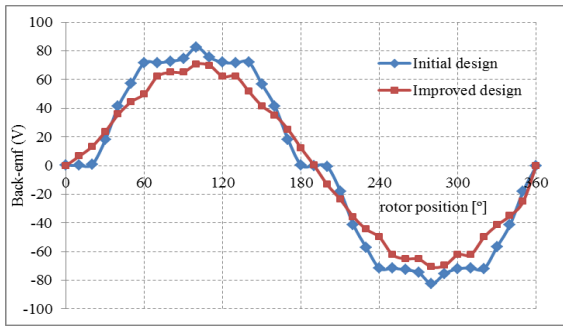


Fig. 9 The fundamental back-emf at 3000 r/min

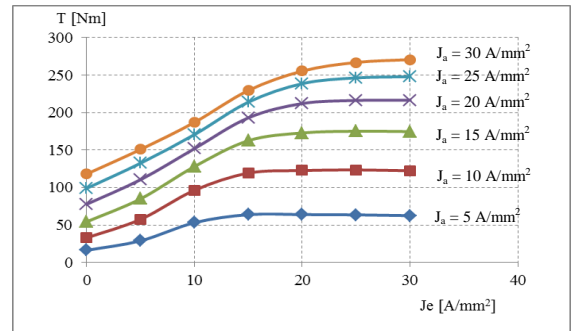


Fig. 13 Torque vs  $J_e$  at various  $J_a$

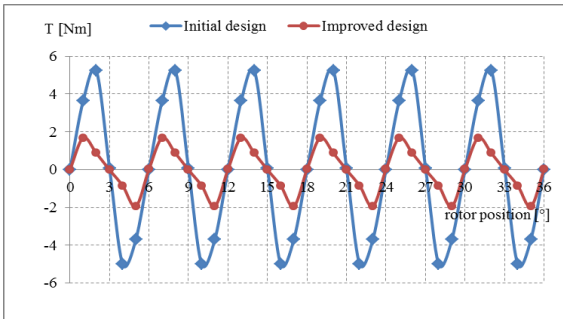


Fig. 10 Cogging torque of the proposed ORHEFSM

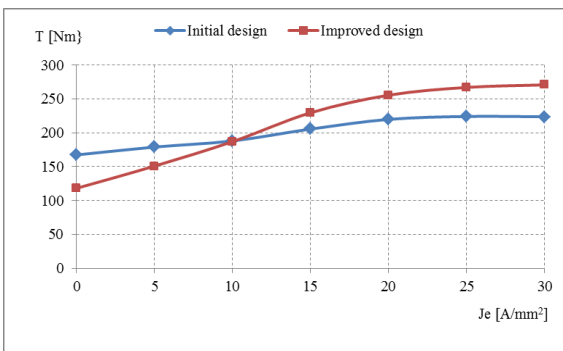


Fig. 11 Torque versus  $J_e$  at maximum  $J_a$

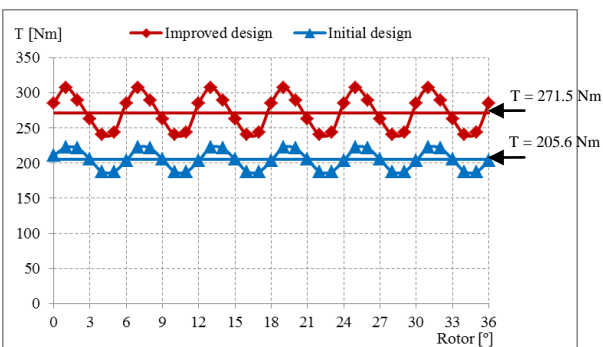


Fig. 12 Average torque of initial and improved design ORHEFSM

## REFERENCES

- [1] J. King, *The King Review of low-carbon cars of low-carbon cars - Part II: recommendations for action*, March 2008. Available at: [www.hm-treasury.gov.uk/king](http://www.hm-treasury.gov.uk/king)
- [2] National Green Technology Policy [Online] Available at: <http://www.kettha.gov.my/en/content/policies-acts-guidelines-1> (Accessed on Jan 2013)
- [3] Review of National Automotive Policy [Online] Available at: <http://www.pekema.org.my> (Accessed on Jan 2013)
- [4] Berita Harian online, Ekonomi "PROTON digesa lebih agresif" 14 Jan 2013 (Accessed on 16 Jan 2013)
- [5] IEA-HEV Outlook, International Energy Agency Implementing Agreement on Hybrid and Electric Vehicles, "Outlook for hybrid and electric vehicles," 2008 [Online] Available: [http://www.ieahev.org/pdfs/iahev\\_outlook\\_2008.pdf](http://www.ieahev.org/pdfs/iahev_outlook_2008.pdf)
- [6] W. Xu, J. Zhu, Y. Guo, S. Wang, Y. Wang, and Z. Shi, "Survey on electrical machines in electrical vehicles," *2009 International Conference on Applied Superconductivity and Electromagnetic Devices*, no. c, pp. 167–170, Sep. 2009.
- [7] W. Fei, P. Luk, and K. Jinpun, "A New Axial flux magnet segmented-armature-torus machine for in-wheel direct drive applications," *IEEE Power Electronics Specialist Conference*, pp. 2197–2202, 2008.
- [8] S. E. Rauch and L. J. Johnson, "Design principles of flux switch alternators," *AIEE Trans.*, vol 74III, no. 12, pp. 1261-1269, 1955.
- [9] Y. Chen, S. Chen, Z.Q. Zhu, D. Howe, and Y.Y. Ye, "Starting torque of single phase flux switching permanent magnet motors," *IEEE Trans. Magn.*, vol 42, no. 10, pp. 3416-3418, 2006.
- [10] E. Hoang, M. Lecrivain, and M. Gabsi, "A New Structure of a Switching Flux Synchronous Polyphased Machine," in *European Conference on Power Electronics and Applications*, no. 33, pp. 1–8, 2007.
- [11] Y. Amara, E. Hoang, M. Gabsi, and M. Lecrivain, "Design and comparison of different flux-switching synchronous machines for an aircraft oil breather application," *Euro. Trans Electr. Power*, no. 15, pp. 497-511, 2005.
- [12] W. Fei, P. Chi, K. Luk and J. S. Y. Wang, "A Novel Outer-Rotor Permanent-Magnet Flux-Switching Machine for Urban Electric Vehicle Propulsion," in *3rd International Conference on Power Electronics Systems and Applications (PESA)*, pp. 1–6, 2009.
- [13] W. Fei, P. Chi, K. Luk, S. Member, J. X. Shen, Y. Wang, and M. Jin, "A Novel Permanent-Magnet Flux Switching Machine With an Outer-Rotor Configuration for In-Wheel Light Traction Applications," *IEEE Transactions on Industry Applications*, vol. 48, no. 5, pp. 1496–1506, 2012
- [14] M.Z. Ahmad, E. Sulaiman, Z.A. Haron, and T. Kosaka, "Preliminary Studies on a New Outer-Rotor Permanent Magnet Flux Switching Machine with Hybrid Excitation Flux for Direct Drive EV Applications", *IEEE Int. Power and Energy Conference (PECON2012)*, pp. 928-933, Dec 2012.